Sensors and Actuators B 238 (2017) 660–666

Contents lists available at ScienceDirect

Sensors and Actuators B: Chemical

journal homepage: www.elsevier.com/locate/snb

Mn-doped ZnS phosphorescent quantum dots: Coumarins optical sensors

Maria E. Pacheco*, Cecilia B. Castells, Liliana Bruzzone

Laboratorio de Investigación y Desarrollo de Métodos Analíticos (LIDMA), Facultad de Ciencias Exactas, Universidad Nacional de La Plata, Calle 47 esq. 115, 1900 La Plata, Argentina

ARTICLE INFO

Article history:
Received 11 February 2016
Received in revised form 14 July 2016
Accepted 22 July 2016
Available online 25 July 2016

Keywords:
Mn-doped ZnS quantum dots
Room temperature phosphorescence
Coumarins
Quenching

ABSTRACT

Mn-doped ZnS quantum dots (QDs) have increasingly attracted much attention as luminescent sensors. Mn^{+2} doping promotes a strong phosphorescence-like emission, allowing the development of novel and highly selective sensing phases. In this vein, a coumarins phosphorescent sensor was developed based on the room temperature phosphorescence quenching of water-soluble Mn-doped ZnS QDs. Phosphorescence lifetimes were measured in order to clarify the involved quenching mechanism. Warfarin determination in pharmaceutical products was performed, reaching good figures of merit. The developed methodology is an alternative, rapid, simple, sensitive and selective method for coumarins determination in pharmaceutical and toxicological samples.

1. Introduction

Coumarins are natural compounds that exhibit a varied biological activity. Warfarin, (RS)-4-Hydroxy-3-(3-oxo-1-phenylbutyl)-2H-chromen-2-one, is used as anticoagulant and, due to the bleeding death caused by the lowered coagulant factors, it is also used as rodenticide; coumarin, 2H-chromen-2-one, is used as an aroma enhancer and as a precursor molecule in pharmaceutical industry and it is found in natural foodstuffs; dicumarol, 3,3′-methylenebis(4-hydroxy-2H-chromen-2-one), is a naturally occurring anticoagulant derived from coumarin due to the action of species of fungi; umbelliferone, 7-Hydroxychromen-2-one, has antioxidant properties and is used in sunscreens. Molecular structures of these coumarins are shown in Fig. 1.

Several analytical methods for coumarins determination were reported in the literature, mostly chromatographic methods [1–34], whereas little work has been done in relation to electrochemical [35–39], capillary electrophoresis [40–42], spectrophotometric [43] and luminescence [11,30,44–55] determination methods. Generally, these analytical techniques are time-consuming, require sophisticated equipment and, consequently, not routinely applicable in quality control laboratories. Besides this, the general trend is towards analytical methodologies that ensure low detection limits. Therefore, there is a need for the development of a rapid, simple, sensitive and selective method for coumarins determination in pharmaceutical and toxicological samples.

With the advent of nanotechnology, conventional organic fluorophores are being replaced by luminescent nanomaterials, such as quantum dots, which have high potential in the development of novel analytical methodologies. Quantum dots (QDs) are nanocrystals of semiconductor materials, with particle size between 2 and 10 nm, exhibiting remarkable optoelectronic properties attributable to quantum confinement effects. High luminescence quantum yields, narrow and symmetric size-tuneable emission spectra and sensitiveness to surface states are some of the unique properties that allow the use of quantum dots for direct (and simple) sensing of different kinds of analytes [56].

Mn-doped ZnS QDs have increasingly attracted much attention as luminescent sensors since Mn^{+2} doping promotes a strong phosphorescence-like emission centred around 590 nm Mn^{+2} ions may act as recombination centres for the excited electron–hole pairs resulting in a strong and characteristic luminescence at longer wavelengths. Room temperature phosphorescence (RTP) has many advantages towards fluorescence: longer Stokes shift between excitation and emission wavelengths, luminescent lifetimes in the order of milliseconds, minimum (almost cero) interference from other concomitant fluorescent compounds and removal of scattered light. These properties, typical from phosphorescent emission, are not encountered in traditional QDs such as CdS, CdSe or ZnS. Additionally, the absence of Cd^{2+} can minimize toxicity due to the eventual release of such toxic metal ions from the nanocrys-

* Corresponding author.
E-mail address: mepacheco@quimica.unlp.edu.ar (M.E. Pacheco).

http://dx.doi.org/10.1016/j.snb.2016.07.125
0925-4005/

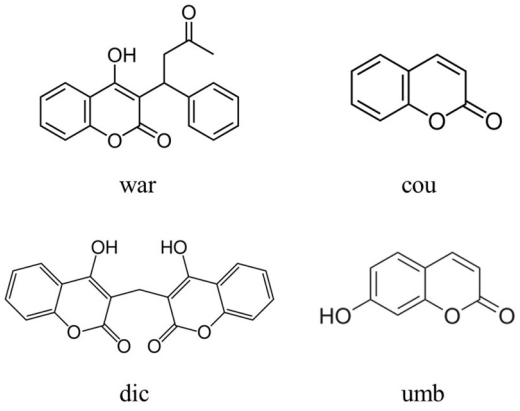

Fig. 1. Molecular structure of coumarins: warfarin (war), coumarin (cou), dicumarol (dic) and umbelliferone (umb).

tals, particularly important in live-experiments. These advantages turn Mn-doped ZnS QDs into attractive analytical luminescent nanomaterials for imaging and sensing. Furthermore, an improvement in selectivity is reached as factors that commonly affect classical phosphorescence emission (presence of heavy atoms or dissolved oxygen, rigid media, etc.) have no influence on the luminescence emission of Mn-doped ZnS QDs [57].

In the present study, Mn-doped ZnS QDs surface-capped with L-cysteine (L-cys) are synthesized. L-cys capping provides water solubility and biocompatibility to the QDs, making them potential sensors for water-soluble analytes in biological samples. Coumarins interaction with Mn-doped ZnS QDs is studied in terms of RTP quenching. The proposed methodology is applied to the determination of warfarin in pharmaceutical products.

2. Experimental

2.1. Reagents and chemicals

All chemicals were analytical-reagent grade and used as received or purificated through conventional procedures. Zinc acetate was acquired from Mallinckrodt. Manganese chloride was supplied by Analar. L-cystein-hydrochloride monohydrate and naphthalene were obtained from Fluka AG Buchs SG. Thioacetamide was provided by Carbo Erba. Warfarin (war), umbelliferone (umb), L-tryptophan, tryptamine hydrochloride, β-naphthol, phenanthrene and anthracene were purchased from Sigma-Aldrich. Rhodamine B was acquired from BDH Chemicals Ltd. Coumarin (cou) and dicumarol (dic) were provided by a local supplier. OmniSolv methanol and absolute ethanol were acquired from Merck. Double-distilled water was used.

QDs, coumarin and umbelliferone phosphate buffer (pH = 7.4) stock solutions and warfarin methanolic stock solutions were prepared daily. A dicumarol standard solution was prepared daily in 0.1 M NaOH. From these solutions, more diluted buffer working solutions were prepared. In the case of warfarin, more diluted buffer/methanol dissolutions were prepared maintaining methanol percentage constant (8% v/v) in the working solutions.

2.2. Instrumentation

Photoluminescence (PL) spectra were carried out on a Perkin-Elmer LS–50 B luminescence spectrometer equipped with a pulsed xenon lamp (10 μs half-width, 60 Hz), an R928 photomultiplier tube and a computer working with FL Winlab software. Fluorescence measurements were performed in a 1.0 cm pathlength quartz cuvette. Front-face room temperature phosphorescence measurements were performed using the front-face accessory and 1.0 cm pathlength cylindrical quartz cuvette of the same diameter of the powder holder. Excitation and emission bandwidths were set at 15 and 20 nm, respectively. A gate time of 5.00 ms and a delay time of 0.10 ms were used for the RTP measurements. QDs excitation wavelength was set at 276 nm and phosphorescence intensities were measured at 584 nm.

Absorption spectra were measured on a Shimadzu UV-240 recording spectrophotometer, equipped with a 1.0 cm pathlength quartz cuvette.

X-ray diffraction patterns (XRD) were obtained on a Philips X-ray diffractometer equipped with a PW 1732/20 generator and a PW 1050/70 goniometer using Cu Kα radiation (λ = 0.15406 nm) at 40 kV and 40 mA. The scan range was 2θ = 15–65° (step scan mode; step size 0.040°; scan speed 1°/min).

2.3. Synthesis of Mn^{+2} doped ZnS QDs

Water-soluble Mn^{+2} doped ZnS QDs capped with L-cys were synthesized following a slightly modified procedure described by Sotelo et al. [57].

Briefly, the capping agent (L-cys) and the precursors (Zn^{+2}, Mn^{+2}) were mixed in a beaker and the pH value was adjusted to 11 using NaOH. The reactant mixture was placed in a three-necked flask and stirred for 30 min under a nitrogen atmosphere. Then, a thioacetamide solution was swiftly injected into the three-necked flask to allow the nucleation of the nanoparticles. The mixture was stirred for 20 min at room temperature. Afterwards, the solution was aged at 50 °C under air atmosphere for 2 h in order to improve the crystalline structure of the L-cys capped Mn-doped ZnS QDs. Purification process was carried out by precipitation of the nanoparticles with ethanol in a centrifuge at 3600 rpm for 10 min (the procedure was repeated 3 times). Finally, the QDs were dried under vacuum and stored under nitrogen atmosphere as a brown solid powder.

2.4. Analytical considerations for phosphorescence quenching measurements

pH regulation was extremely important due to the presence of pH-dependent molecules (i.e. molecules having ionizable groups that change their absorption properties: L-cys and coumarins). Phosphate buffer (pH = 7.4) was selected for some reasons: is the physiological pH, QDs dissolutions are stable and is the buffer used for warfarin determination (see Section 2.5).

2.5. Analytical procedure for warfarin determination

A warfarin determination was performed in Circuvit 5 mg (Ariston S.A. Laboratory), a commercially sold anticoagulant. The pills were pre-treated following the procedure provided by Ariston S.A. Laboratory. This sample preparation method is analogous to the one reported in the USP36-NF31 [58]. Twenty-five pills were pulverized in an agate mortar with a pestle; 2000 mg of the resulting powder were weighted in a 50.00 mL volumetric flask and 30.0 mL of dilution solvent (phosphate buffer pH = 7.4: acetonitrile, 85:15 v/v) were added. The solution was magnetically stirred for 60 min. The volume was completed with dilution solvent. The resultant solution was filtered through a filter paper (Whatman #41). The 1:5 buffer dilution was made in order to use it as the stock solution. The sample was analyzed in triplicate, at three concentration levels.

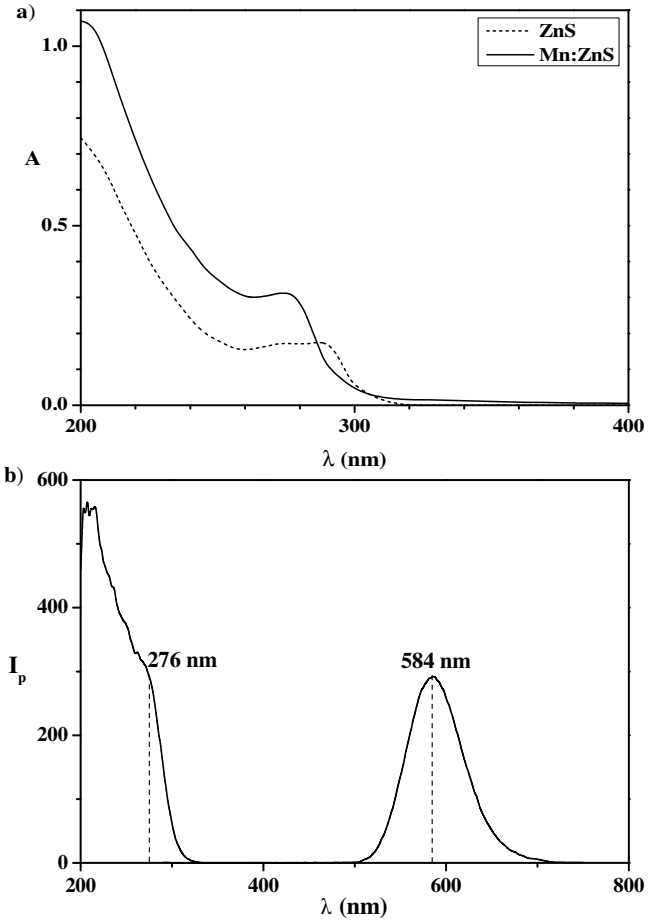

Fig. 2. a) Absorption spectra of ZnS and Mn-doped ZnS QDs. b) Excitation and emission spectra of Mn-doped ZnS QDs.

3. Results and discussion

3.1. Characterization of the as-synthesized Mn-doped ZnS QDs

Absorbance spectrum of Mn-doped ZnS QDs exhibits a shoulder absorption peak at 276 nm. In comparison to ZnS nanoparticles, whose absorption peak is at 290 nm, it is blue-shifted (Fig. 2a). This fact can be attributed to quantum confinement.

Luminescence excitation and emission spectra of a dissolution of Mn-doped ZnS QDs are shown in Fig. 2b. The phosphorescence emission can be attributed to the doping of Mn^{+2} into the ZnS lattice. After excitation, the energy is transferred from the excited energy levels of the semiconductor material to the excited energy levels of Mn^{+2}. The deactivation process occurs through the well-known d–d transition of manganese ($^4T_1$-$^6A_1$). As this transition is spin forbidden, Mn-doped ZnS QDs shows a delayed luminescence that presents typical properties of a phosphorescence-like emission: large Stokes shift between excitation and emission wavelengths (308 nm) and long luminescent lifetimes (in the order of a few ms –see Section 3.3).

The photoluminescence quantum yield (PL-QY) value of Mn-doped ZnS QDs was determined using the following equation:

$$QY_{sample} = \left(\frac{F_{sample}}{F_{ref}}\right)\left(\frac{A_{ref}}{A_{sample}}\right)\left(\frac{n^2_{sample}}{n^2_{ref}}\right) QY_{ref}$$

where F is the area under the emission spectrum, A is the absorbance value at the excitation wavelength and n is the refractive index. Rhodamine B in ethanol was used as reference (QY = 0.73 [59]). Mn-doped ZnS QDs emission spectrum integration was performed taking into account the isolated emission band at long wavelengths corresponding to the $^4T_1$-$^6A_1$ d–d transition of Mn^{+2}. The PL-QY determined value was 0.0003.

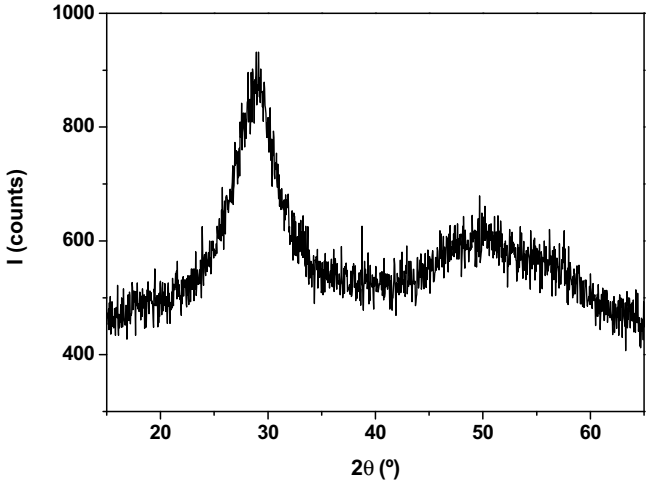

Fig. 3. XRD diffraction patterns of Mn-doped ZnS QDs.

XRD patterns are shown in Fig. 3; the broadened nature confirms the formation of small sized nanoparticles. In order to estimate the average crystallite size (D), the Debye-Scherer formula [60] was used:

$$D = \frac{K\lambda}{\beta\, cos\theta}$$

where λ is the X-ray wavelength of Cu Kα radiation (0.15406 nm), β is the full width at half maxima (FWHM) of the most prominent peak in radians, θ is the Bragg diffraction angle and K can be taken as equals to 0.9 for spherical particles. The estimated average crystallite size of Mn-doped ZnS QDs was found to be 2.7 nm.

3.2. Phosphorescence quenching of Mn-doped ZnS QDs by coumarins

Luminescence properties of QDs strongly depend on the interaction between their surface and different chemical species [56,61]. The sensitivity to changes in their surface and environment is the foundation for the development of novel optical sensors based on QDs probes. In this vein, the possible optical sensing of coumarins was investigated by means of its interaction with Mn-doped ZnS QDs.

The addition of increasing amounts of coumarins efficiently quenches the RTP of Mn-doped ZnS QDs. Optimization of QDs concentration was performed in order to obtain the major difference between phosphorescence intensity in presence and absence of coumarins (I_o-I). Warfarin was used as model coumarin. Optimum Mn-doped ZnS QDs concentration was 20 ppm under the studied conditions, reaching a committed relationship between major difference and absorption values – inner filter effects – (Fig. 4). Percentage of methanol was optimized in the case of warfarin, leading to an optimum value of 8% v/v (Fig. 5). The observed RTP quenching can be explained in terms of the classical Stern-Volmer equation (Fig. 6). Data points are duplicates at the same concentration level obtained from independent solutions, except from the extremes and middle concentrations where data points are triplicates. Previous works [54,62] have demonstrated that there are noticeable differences between RTP measurements at right-angle and front-face illumination geometry when coumarins are under study due to inner filter effects. In order to overcome these effects, front-face

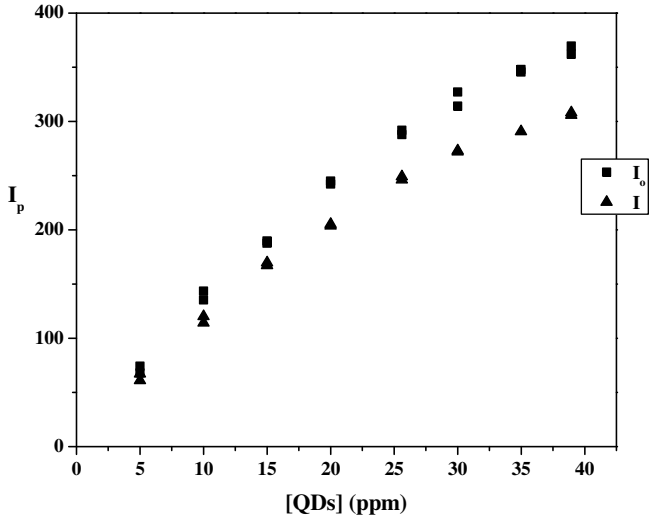

Fig. 4. Mn-doped ZnS QDs optimization. [war] = 3.00×10^{-5} M; 8% v/v methanol; buffer pH 7.4.

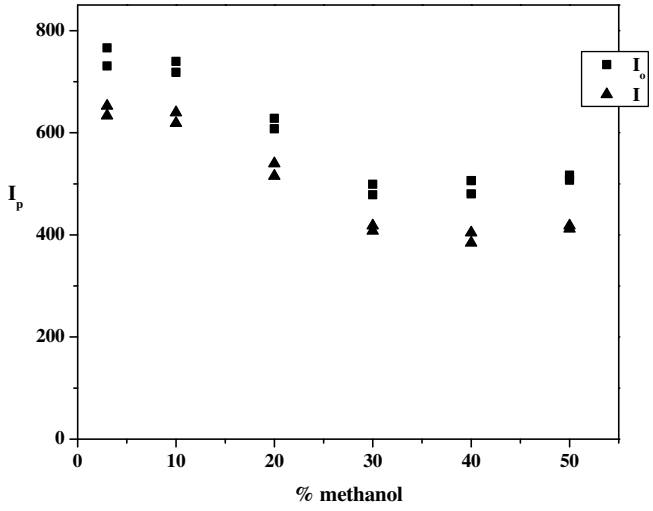

Fig. 5. Methanol optimization. [QDs] = 20 ppm; [war] = 3.00×10^{-5} M; buffer pH 7.4.

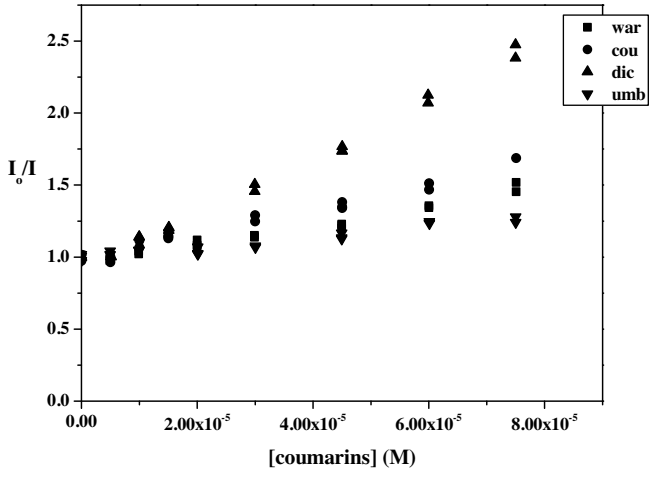

Fig. 6. Stern-Volmer plots for coumarins quenching of QDs. [QDs] = 20 ppm.

Table 1
Molar extinction coefficients.

	ε (M^{-1} cm^{-1}) 276 nm	Combined standard uncertainty[a]
war	9433	238
cou	11100	168
dic	10117	189
umb	3537	197

[a] Estimated standard deviation equal to the positive square root of the total variance obtained by combining all the uncertainty components using the law of propagation of uncertainty.

Table 2
Stern-Volmer constant values.

	K_{SV} (M^{-1})
QDs:war	4937 ± 583
QDs:cou	7967 ± 631
QDs:dic	16865 ± 961
QDs:umb	3547 ± 529

illumination geometry is used in all measurements. The slightly upward curvature seen in the figures is explained in terms of the absorption characteristics of the studied compounds (Table 1); as the concentration increases, the inner filter effects becomes more important and even at front-face illumination geometry a loose of linearity can be observed. Table 2 summarizes the values of the Stern-Volmer constants (Ksv) for each compound, obtained from the Stern-Volmer plots in the linear region.

The quenching mechanism is discussed in the next section, but up to this point the studied interaction between QDs and coumarins seems to be a potential methodology in coumarins optical sensing.

3.3. Quenching mechanism

Static and dynamic quenching can be distinguished by their differing dependence on temperature and viscosity, changes in the absorption spectra or preferably by lifetime measurements [59,63].

In order to confirm the involved quenching mechanism, phosphorescence lifetimes were measured at front-face illumination geometry. A gate time of 1.00 ms and a varied delay time were used, setting the excitation and emission wavelength at 276 and 584 nm, respectively. The decay curves have been fitted using a double exponential time course with two components, the first one (τ_1) within the range of 0.7 ms and the second one (τ_2) around 2.7 ms. For Mn-doped ZnS QDs, the first lifetime component has been attributed to different processes like fluorescent deactivation of the ZnS host or surface-exposed Mn^{2+} ions. The second slowest component is related to the emission via dopant energy levels [64]. As phosphorescence emission is being analyzed, the second component of the lifetime is taking into account. Fig. 7 shows the Stern-Volmer plots in terms of phosphorescence lifetime for the RTP quenching of QDs. It can be noted that there is a negligible variation in the ratio τ_o/τ with quencher concentration indicating that the quenching mechanism is static. Static quenching removes a fraction of the phosphorophores from observation. The complexed phosphorophores are nonluminescent, and the only observed phosphorescence is from the uncomplexed phosphorophores. The uncomplexed fraction is unperturbed, and, hence, the lifetime is τ_o. Therefore, for static quenching $\tau_o/\tau = 1$. In contrast, for dynamic quenching $I_o/I = \tau_o/\tau$. The decrease in lifetime occurs because quenching is an additional rate process that depopulates the excited state [59,63]. A possible explanation for the static quenching is the formation of an imine complex between the carbonyl group of the coumarins and the amino group of L-cysteine [57].

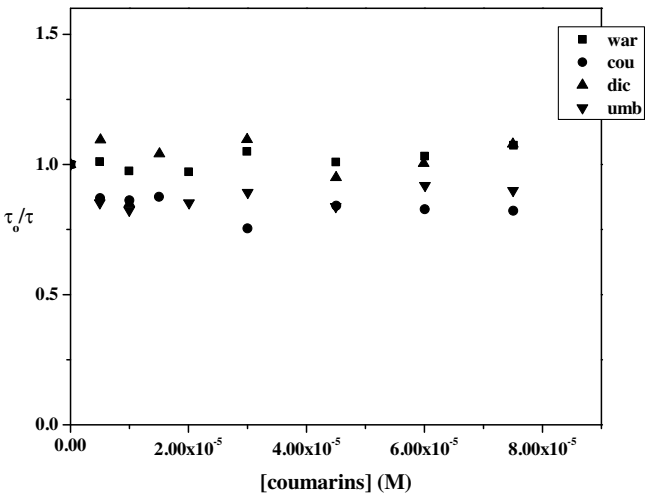

Fig. 7. Stern-Volmer plots in terms of phosphorescence lifetime for the RTP quenching of QDs. [QDs] = 20 ppm.

Table 3
Figures of merit[1] for the determination of warfarin by RTP quenching of QDs.

	$I_o/I = a + b[war]$		
a	0.995	s_a	0.004
b	5417 M^{-1}	s_b	134 M^{-1}
$s_{y/x}$	0.008		
r	0.997		
SEN	5417 M^{-1}		
γ	6.87×10^5 M^{-1}		
LOD	4.71×10^{-6} M		
LOQ	1.07×10^{-5} M		
Dynamic Range	4.71×10^{-6} M – 4.50×10^{-5} M		
Linear Range	1.07×10^{-5} M – 4.50×10^{-5} M		

[1] a (intercept), s_a (standard error of the intercept), b (slope), s_b (standard error of the slope), $s_{y/x}$ (standard error of the regression), r (correlation coefficient). Figures of merit: SEN (calibration sensitivity), γ (analytical sensitivity), LOD (limit of detection), LOQ (limit of quantification). $LOD = 2 \times t_{0.05;N-2} \times s_0$; $LOQ = 10 \times s_0$; $s_0 = \frac{s_{y/x}}{b}\sqrt{\frac{1}{\sum_i n_i} + \frac{1}{m} + \frac{\bar{x}^2}{\sum_i (x_i - \bar{x})^2}}$ [65].

3.4. Warfarin determination in pharmaceuticals

Warfarin concentration found was 4.9 ± 0.1 mg per pill under the optimized conditions. It was in agreement with the concentration reported by the laboratory and fits the USP36-NF31 requirements (warfarin sodium tablets contain not less than 95.0 percent and not more than 105.0 percent of the labeled amount of warfarin sodium) [58]. No interference due to the excipients was observed. Table 3 summarizes the figures of merit of the proposed method.

3.4.1. Selectivity

The response of Mn-doped ZnS QDs to other molecules (interferences) was examined in order to evaluate the selectivity of the studied QDs to warfarin. RTP intensity of QDs and warfarin in presence (I) and absence (I_o) of the interference was measured. An equimolar concentration of warfarin and interference was used. Fig. 8 displays the variation of the ratio I_o/I for the different molecules under evaluation. As can be observed, Mn-doped ZnS QDs exhibit a high selectivity to warfarin: the ratio I_o/I is almost the same in presence of a concomitant molecule.

4. Conclusions

The interaction between phosphorescent quantum dots and coumarins was studied in terms of a room temperature phosphorescence quenching. In order to overcome undesirable inner filter effects, front-face illumination geometry was used. Stern-Volmer constants were calculated in the linear region. Phosphorescence lifetimes were measured at different coumarins concentration leading to a static quenching mechanism. An alternative analytical method for the determination of warfarin in commercial products was performed with good figures of merit.

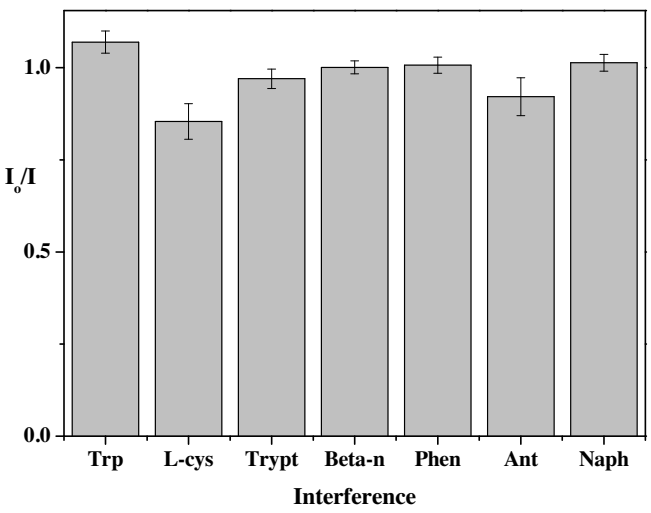

Fig. 8. RTP intensity of QDs and warfarin in presence (I) and absence (I_o) of the interference. [QDs] = 20 ppm; [war] = [interference] = 2.00×10^{-5} M; buffer pH 7.4/methanol (8% v/v). Interferences: L-tryptophan (Trp), L-cystein (L-cys), tryptamine (Trypt), β-naphthol (Beta-n), phenanthrene (Phen), anthracene (Ant) and naphthalene (Naph).

Acknowledgments

The authors thank Facultad de Ciencias Exactas, Universidad Nacional de La Plata, Argentina, and Consejo Nacional de Investigaciones Científicas y Técnicas (CONICET) for partial financial support. M. E. P. is a fellow of CONICET.

References

[1] C.W. Loomis, W.J. Racz, Determination of warfarin in plasma by gas-liquid chromatography, Anal. Chim. Acta 106 (1979) 155–159.
[2] M. Ueland, G. Kvalheim, P.E. Lønning, S. Kvinnsland, Determination of warfarin in human plasma by high performance liquid chromatography and photodiode array detector, Ther. Drug Monit. 7 (1985) 329–335.
[3] J.M. Steyn, H.M. Van Der Merwe, Reversed-phase high-performance liquid chromatographic method for the determination of warfarin from biological fluids in the low nanogram range, J. Chromatogr. 378 (1986) 254–269.
[4] Y.W.J. Wong, P.J. Davis, Analysis of warfarin and its metabolites by reversed phase ion-pair liquid chromatography with fluorescence detection, J.Chromatogr. 469 (1989) 281–291.
[5] J. Dalbacke, I. Dahlquist, C. Persson, Determination of warfarin in drinking water by high performance liquid chromatography after solid-phase extraction, J. Chromatogr. A 507 (1990) 381–387.
[6] S. Sharifz, H.C. Michaelis, E. Lotterer, J. Bircher, Determination of coumarin 7-Hydroxy-Coumarin, 7-Hydroxycoumarin- glucuronide, and 3-Hydroxycoumarin by high-performance liquid chromatography, J. Liq. Chromatogr. 16 (1993) 1263–1278.
[7] H. Takahashi, T. Kashima, S. Kimura, N. Muramoto, H. Nakahata, S. Kubo, Y. Shimoyama, M. Kajiwara, H. Echizen, Determination of unbound warfarin enantiomers in human plasma and 7-hydroxywarfarin in human urine by chiral stationary-phase liquid chromatography with ultraviolet or fluorescence and on-line circular dichroism detection, J. Chromatogr. B 701 (1997) 71–80.
[8] A. Medvedovici, F. David, P. Sandra, Determination of the rodenticides warfarin, diphenadione and chlorophacinone in soil samples by HPLC-DAD, Talanta 44 (1997) 1633–1640.
[9] H. Pouliquen, V. Fauconnet, M.-L. Morvan, L. Pinault, Determination of warfarin in the yolk and the white of hens' eggs by reversed-phase high-performance liquid chromatography, J. Chromatogr. B 702 (1997) 143–148.

[10] D. De Orsi, L. Gagliardi, L. Turchetto, D. Tonelli, HPLC determination of warfarin and acenocoumarol in raw materials and pharmaceuticals, J. Pharm. Biomed. Anal. 17 (1998) 891–895.
[11] M.E. Fernández Izquierdo, J. Quesada Granados, M. Villalón Mir, M.C. López Martinez, Comparison of methods for determining coumarins in distilled beverages, Food Chem. 70 (2000) 251–258.
[12] P.R. Ring, J.M. Bostick, Validation of a method for the determination of (*R*)-warfarin and (*S*)-warfarin in human plasma using LC with UV detection, J. Pharm. Biomed. Anal. 22 (2000) 573–581.
[13] R.M.S. Celeghini, J.H.Y. Vilegas, Fernando M. Lanças, Extraction and quantitative HPLC analysis of coumarin in hydroalcoholic extracts of Mikania Glomerata Spreng. (guaco) leaves, J. Braz. Chem. Soc. 12 (2001) 706–709.
[14] V.K. Boppana, W.H. Schaefer, M.J. Cyronak, High-performance liquid-chromatographic determination of warfarin enantiomers in plasma with automated on-line sample enrichment, J. Biochem. Biophys. Methods 54 (2002) 315–326.
[15] M.U.B. Kammerer, J. Kirchheiner, A. Rane, J.-O. Svensson, Determination of phenprocoumon, warfarin and their monohydroxylated metabolites in human plasma and urine by liquid chromatography-mass spectrometry after solid-phase extraction, J. Chromatogr. B 809 (2004) 217–226.
[16] I. Locatelli, V. Kmetec, A. Mrhar, I. Grabnar, Determination of warfarin enantiomers and hydroxylated metabolites in human blood plasma by liquid chromatography with achiral and chiral separation, J. Chromatogr. B 818 (2005) 191–198.
[17] A. Osman, K. Arbring, T.L. Lindahl, A new high-performance liquid chromatographic method for determination of warfarin enantiomers, J. Chromatogr. B 826 (2005) 75–80.
[18] L.S. de Jager, G.A. Perfetti, G.W. Diachenko, Determination of coumarin, vanillin, and ethyl vanillin in vanilla extract products: liquid chromatography mass spectrometry method development and validation studies, J. Chromatogr. A 1145 (2007) 83–88.
[19] G. Vecchione, B. Casetta, M. Tomaiuolo, E. Grandone, M. Margaglione, A rapid method for the quantification of the enantiomers of warfarin, phenprocoumon and acenocoumarol by two-dimensional-enantioselective liquid chromatography/electrospray tandem mass spectrometry, J. Chromatogr. B 850 (2007) 507–514.
[20] C. Sproll, W. Ruge, C. Andlauer, R. Godelmann, D.W. Lachenmeier, HPLC analysis and safety assessment of coumarin in foods, Food Chem. 109 (2008) 462–469.
[21] J. Su, C. Zhang, W. Zhang, Y.-H. Shen, H.-L. Li, R.-H. Liu, X. Zhang, X.-J. Hub, W.-D. Zhang, Qualitative quantitative determination of the major coumarins in Zushima by high performance liquid chromatography with diode array detector mass spectrometry, J. Chromatogr A. 1216 (2009) 2111–2117.
[22] J. Malakova, P. Pavek, L. Svecova, I. Jokesova, P. Zivny, V. Palicka, New high-performance liquid chromatography method for the determination of (*R*)-warfarin and (*S*)-warfarin using chiral separation on a glycopeptide-based stationary phase, J. Chromatogr. B 877 (2009) 3226–3230.
[23] Z. Zuo, S.K. Wo, C.M.Y. Lo, L. Zhou, G. Cheng, J.H.S. You, Simultaneous measurement of S-warfarin, R-warfarin, S-7-hydroxywarfarin and R-7-hydroxywarfarin in human plasma by liquid chromatography-tandem mass spectrometry, J. Pharm. Biomed. Anal. 52 (2010) 305–310.
[24] M. Hadjmohammadi, H. Ghambari, Three-phase hollow fiber liquid phase microextraction of warfarin from human plasma and its determination by high-performance liquid chromatography, J. Pharm. Biomed. Anal. 61 (2012) 44–49.
[25] H. Ghambari, M. Hadjmohammadi, Low-density solvent-based dispersive liquid–liquid microextraction followed by high performance liquid chromatography for determination of warfarin in human plasma, J. Chromatogr. B 899 (2012) 66–71.
[26] N.A. Siddique, M. Mujeeb, M. Aamir, A. Husain, Simultaneous quantification of umbelliferone and quercetin in polyherbal formulations of Aegle Marmelos by HPTLC, Am. J. Pharm Tech. Res. 2 (2012) 568–577.
[27] H.M. Marwani, E.M. Bakhsh, Silica gel supported hydrophobic ionic liquid for selective extraction and determination of coumarin, Am. J. Anal. Chem. 4 (2013) 8–16.
[28] K. Hroboňová, A. Spevak, Ľ. Spišská, J. Lehotay, J. Čižmárik, Application of umbelliferone molecularly imprinted polymer in analysis of plant samples, Chem. Papers 67 (2013) 477–483.
[29] Y.-H. Wang, B. Avula, N.P.D. Nanayakkara, J. Zhao, I.A. Khan, Cassia cinnamon as a source of coumarin in cinnamon-flavored food and food supplements in the United States, J. Agric. Food Chem. 61 (2013) 4470–4476.
[30] K. Hrobonňová, J. Lehotay, J. Čižmárik, J. Sádecká, Comparison HPLC and fluorescence spectrometry methods for determination of coumarin derivatives in propolis, J. Liq. Chromatogr. Relat. Technol. 36 (2013) 486–503.
[31] T. Lomonaco, S. Ghimenti, I. Piga, M. Onor, B. Melai, R. Fuoco, F. Di Francesco, Determination of total and unbound warfarin and warfarin alcohols in human plasma by high performance liquid chromatography with fluorescence detection, J. Chromatogr. A 1314 (2013) 54–62.
[32] Y. Shen, C. Han, B. Liu, Z. Lin, X. Zhou, C. Wang, Z. Zhu, Determination of vanillin, ethyl vanillin and coumarin in infant formula by liquid chromatography-quadrupole linear ion trap mass spectrometry, J. Dairy Sci. 97 (2014) 679–686.
[33] F. Ahmadi, E. Yawari, M. Nikbakht, Computational design of an enantioselective molecular imprinted polymer for the solid phase extraction of S-warfarin from plasma, J. Chromatogr. A 1338 (2014) 9–16.
[34] O.Y. Alshogran, A.J. Ocquea, J. Zhao, B.W. Day, F.A. Leblond, V. Pichetted, T.D. Nolin, Determination of warfarin alcohols by ultra-high performance liquid chromatography–tandem mass spectrometry: application to in vitro enzyme kinetic studies, J. Chromatogr. B 944 (2014) 63–68.
[35] M.M. Ghoneim, A. Tawfik, Assay of anti-coagulant drug warfarin sodium in pharmaceutical formulation and human biological fluids by square-wave adsorptive cathodic stripping voltammetry, Anal. Chim. Acta 511 (2004) 63–69.
[36] S.S.M. Hassan, W.H. Mahmoud, M.A.F. Elmosallamy, M.H. Almarzooqi, Iron(II)-phthalocyanine as a novel recognition sensor for selective potentiometric determination of diclofenac and warfarin drugs, J. Pharm. Biomed. Anal. 39 (2005) 315–321.
[37] L.-H. Wang, H.-H. Liu, Electrochemical reduction of coumarins at a film-modified electrode and determination of their levels in essential oils and traditional chinese herbal medicines, Molecules 14 (2009) 3538–3550.
[38] D.M. Miyano, T. Lima, F.R. Simões, M.A. La-Scalea, H.P.M. Oliveira, L. Codognoto, Electrochemical study of simple coumarin and its determination in aqueous infusion of Mikania glomerata, J. Braz. Chem. Soc. 25 (2014) 602–609.
[39] B. Rezaei, O. Rahmanian, A.A. Ensafi, An electrochemical sensor based on multiwall carbon nanotubes and molecular imprinting strategy for warfarin recognition and determination, Sens. Actuators B Chem. 196 (2014) 539–545.
[40] P. Gareil, Separation and determination of warfarin enantiomers in human plasma samples by capillary zone electrophoresis using a methylated/I-cyclodextrin-containing electrolyte, J.Chromatogr 615 (1993) 317–325.
[41] Q. Zhou, W.-P. Yau, E. Chan, Enantioseparation of warfarin and its metabolites by capillary zone electrophoresis, Electrophoresis 24 (2003) 2617–2626.
[42] M. Wang, Z. Cai, L. Xu, Coupling of acetonitrile deproteinization and salting-out extraction with acetonitrile stacking in chiral capillary electrophoresis for the determination of warfarin enantiomers, J. Chromatogr. A 1218 (2011) 4045–4051.
[43] C.S.P. Sastry, T. Thirupathi Rao, A. Sailaja, J. Venkateswara Rao, Micro-determination of warfarin sodium, nicoumalone and acebutolol hydrochloride in pharmaceutical preparations, Talanta 38 (1991) 1107–1109.
[44] H.C. Hollifield, J.D. Winefordner, Fluorescence and phosphorescence characteristics of anticoagulants. A new approach to direct measurement of drugs in whole blood, Talanta 14 (1967) 103–107.
[45] S.Y. Su, E. Asafu-Adjaye, S. Ocak, Room-temperature phosphorimetry of pesticides using a luminescence sampling system, Analyst 109 (1984) 1019–1023.
[46] F. Garcia Sánchez, C. Cruces Blanco, Synchronous derivative room-temperature phosphorescence determination of warfarin in blood serum, Anal. Chim. Acta 222 (1989) 177–188.
[47] S. Panadero, A. Gómez-Hens, D. Pérez-Bendito, Simultaneous determination of warfarin and bromadiolone by derivative synchronous fluorescence spectrometry, Talanta 40 (1993) 225–230.
[48] P. Solich, M. Polášek, R. Karlíček, Sequential flow-injection spectrofluorimetric determination of coumarins using a double-injection single-line system, Anal. Chim. Acta 308 (1995) 293–298.
[49] S. Ishiwata, M. Kamiya, Cyclodextrin inclusion effects on fluorescence and fluorimetric properties of the pesticide warfarin, Chemosphere 34 (1997) 783–789.
[50] L.F. Capitán-Vallvey, M.K.A. Deheidel, R. Avidad, Determination of warfarin in waters and human plasma by Solid-Phase Room-Temperature Transmitted Phosphorescence, Arch. Environ. Contam. Toxicol. 37 (1999) 1–6.
[51] R. Badía, M.E. Díaz-García, Cyclodextrin-based optosensor for the determination of warfarin in waters, J. Agric. Food Chem. 47 (1999) 4256–4260.
[52] G. de Armas, M. Miró, J.M. Estela, V. Cerdà, Multisyringe flow injection spectrofluorimetric determination of warfarin at trace levels with on-line solid-phase preconcentration, Anal. Chim. Acta 467 (2002) 13–23.
[53] Z. Chang, H.-T. Yan, Cloud point extraction-fluorimetric combined methodology for the determination of trace warfarin based on the sensitization effect of supramolecule, J.Lumin 132 (2012) 811–817.
[54] M.E. Pacheco, L. Bruzzone, Room temperature phosphorescence quenching study of coumarins. Indirect determination of warfarin in pharmaceuticals, Anal. Methods 6 (2014) 3462–3466.
[55] A. Dehbozorgi, J. Tashkhourian, S. Zare, Fluorescence determination of warfarin using TGA-capped CdTe quantum dots in human plasma samples, J. Fluoresc. 25 (2015) 1887–1895.
[56] J.M. Costa-Fernández, R. Pereiro, A. Sanz-Medel, The use of luminescent quantum dots for optical sensing, Trends Anal. Chem. 25 (2006) 207–218.
[57] E. Sotelo-Gonzalez, M.T. Fernandez-Argüelles, J.M. Costa-Fernández, A. Sanz-Medel, Mn-doped ZnS quantum dots for the determination of acetone by phosphorescence attenuation, Anal. Chim. Acta 712 (2012) 120–126.
[58] United States Pharmacopeia (USP)—National Formulary (NF), 36 (2013) 5588.
[59] C.A. Parker, Photoluminescence of Solutions, Elsevier Publishing Company, Amsterdan, 1968.
[60] A.K. Kole, C.S. Tiwary, P. Kumbhakar, Room temperature synthesis of Mn^{2+} doped ZnS d-dots and observation of tunable dual emission: effects of doping concentration, temperature, and ultraviolet light illumination, J. Appl. Phys. 113 (2013) 114308-1–114308-11.
[61] Y. Lou, Y. Zhao, J. Chena, J. Zhu, Metal ions optical sensing by semiconductor quantum dots, J. Mater. Chem. C 2 (2014) 595–613.

[62] M.E. Pacheco, L. Bruzzone, Room temperature phosphorescence of the 1-bromonaphthalene/β-cyclodextrin inclusion complex: comparison between right-angle and front-face illumination geometry, Anal. Methods 5 (2013) 6908–6910.
[63] J.R. Lakowicz, Principles of Fluorescence Spectroscopy, third ed., Springer Publisher, New York, 2006.
[64] E. Sotelo-Gonzalez, L. Roces, S. García-Granda, M.T. Fernandez-Argüelles, J.M. Costa-Fernández, A. Sanz-Medel, Influence of Mn^{2+} concentration on Mn^{2+}-doped ZnS quantum dot synthesis: evaluation of the structural and photoluminescent properties, Nanoscale 5 (2013) 9156–9161.
[65] H.C. Goicoechea, A.C. Olivieri, La Calibración En Química Analítica, first ed., Universidad Nacional del Litoral, Santa Fe, 2007.

Biographies

Maria E. Pacheco received her BS degree in Analytical Chemistry in 2011 from the National University of La Plata (UNLP), Argentina. Currently, she is a PhD student at the Analytical Chemistry Division of the Exact Sciences Faculty, UNLP, supervised by Prof. Dr. Cecilia Castells and Prof. Dr. Liliana Bruzzone. She was awarded with a doctoral fellowship from the Argentine Research Council (CONICET). Her doctoral thesis focuses on the development and application of photoluminescent analytical methodologies for coumarins sensing. She acts as a Teaching Assistant at the Analytical Chemistry Division of the mentioned Faculty.

Cecilia B. Castells is full professor of Separation Science and director of LIDMA at the National University of La Plata (UNLP), Argentina. She received her PhD in Biochemistry from UNLP (1994) and was research associate at the University of Minnesota. She was visiting professor at the University of Barcelona, University of Valencia and taught a master's course at the Gdansk University of Technology. Her research activities concern the theoretical fundamentals of several separative techniques and the study of the equilibria associated with those methods, the thermodynamics of gas chromatography and liquid chromatography, and the development of chiral separation methods.

Liliana Bruzzone received her PhD in Analytical Chemistry from the National University of La Plata (UNLP), Argentina, in 1981. She has been teaching Analytical Chemistry at the Exact Sciences Faculty of the mentioned University since 1970. She delivered masterís and postgraduate courses in several opportunities and collaborated in teaching modules of Geochemistry career at Natural Science and Museum Faculty. Her research interests cover luminescence spectrometry, nanomaterials, imprinted polymers and chemical sensors.